A Ray Tracing Method for Geodesic Based Tractography in Diffusion Tensor Images

Neda Sepasian Anna Vilanova Luc Florack
B. M. Ter Haar Romeny
Department of Biomedical Engineering,
Eindhoven University of Technology, PO Box 513, 5600 MB Eindhoven,
The Netherlands {N.Sepasian,A.Vilanova,L.M.J.Florack,B.M.TerHaarRomeney}@tue.nl

Abstract

We present multi-valued solution algorithm for geodesic-based fiber tracking in a tensor-warped space given by diffusion tensor imaging data. This technique is based on solving ordinary differential equations describing geodesics by a ray tracing algorithm. The algorithm can capture all possible geodesics connecting two given points instead of a single geodesic captured by Hamilton-Jacobi based algorithms. Once the geodesics have been computed, using suitable connectivity measures, we can choose among all solutions the most likely connection pathways which correspond best to the underlying real fibrous structures. In comparison with other approaches, our algorithm gives the possibility of applying different cost functions in a fast post-processing. Moreover, the algorithm can be used for capturing possible multi-path connections between two points that can happen when, e.g., pathologies are presented. Synthetic second order diffusion tensor data in a two dimensional space are employed to illustrate the potential applications of the algorithm to fiber tracking.

Keywords. geodesic, diffusion tensor images, fiber tracking, Hamilton-Jacobi equation, ray tracing.

1. Introduction

Diffusion tensor imaging (DTI) is the first non-invasive technique based on magnetic resonance imaging (MRI) that enables the measurement of the restricted diffusion of water molecules in tissues, see for example Basser *et al* [3]. It is possible to calculate, for each voxel, a diffusion tensor which is a symmetric positive definite 3×3 matrix. This matrix describes the three-dimensional diffusivity, [11]. The principal application is in imaging of the brain white matter, where the location, orientation and anisotropy of the fiber tracts can be measured [2]. It is assumed that fiber tracks in brain white matter follow the direction with the largest diffusivity. This means that the time a water molecule travels a given distance in this direction is the shortest.

Many different approaches have been devised for fiber tracking. The most common techniques reduce the information of the tensor to the main eigenvector. The integral lines of the vector field generated by the main eigenvector are used to indicate fiber tracks. However, these methods do not use the full information of the tensor and are very sensitive to noise, see Jun *et al* [6].

Another set of techniques uses the full tensor information by computing geodesics in a Riemannian space with a metric defined by the inverse of diffusion tensor. Early DTI geodesic connectivity approaches are based on solving the standard eikonal equation [4, 8, 16], where connectivity measurements are represented by cost functions of eikonal equation based on the similarity measurements of tensors. The more recent approaches introduce cost functions which consider the directionality as well as the shape of the tensor. For example, Kao *et al* [5] represented a front propagation algorithm based on an anisotropic Hamilton-Jacobi equation in which the front propagation is given by the diffusivity rate in the normal direction of the front.

A third class of algorithms is based on high angular resolution data images (HARDI). For example, Melakons [9, 10] considers the directionality of the diffusion data by applying the cost function depending on the diffusivity directions. In these approaches, in order to overcome the restriction of Riemannian geometry to ellipsoidal diffusion profile, the Finsler metric is used, and a new Hamilton-Jacobi equation is derived by minimizing the given cost function. We con-

centrate on the 2nd order tensor model of diffusion which is still the most commonly used.

A characteristic of Hamilton-Jacobi(HJ) based approaches is that they give only the single-valued viscosity solution corresponding to the minimizer of a cost function. However, this is a limitation. In some cases multiple geodesics or fibers connecting two points. For example, if a "pathology" is present like a tumor that pushes the fibers, it can be multiple paths which are connecting two points. Furthermore, in some studies, like the one by Parker *et al* [13], it is shown that some structures (i.e., Broca and Wernicke) have multiple path connections. Therefore, the HJ approach suffers from the stated deficiency that it singles out a preferred geodesic that does not necessarily correspond to the desired geodesic in case of multiple geodesic connections. Moreover, different cost functions have been developed [1, 14, 8, 9, 16]. Since in different cases, it is not a priori clear which cost function to choose, having the solution of different cost functions may be interesting. However, different cost functions result in different Hamilton-Jacobi equations, and in order to examine several cost functions, one needs to solve several equations, which can be computationally expensive.

In this paper, we present a new geodesic-based algorithm which can be used for fiber tracking in a tensor-warped space. This algorithm computes possible multi-valued solutions using the entire tensor information. Note that between two given points on a manifold, depending on initial directions, there may be more than one geodesic, and therefore multiple solutions may arise. Once the geodesics have been computed, using suitable connectivity measures, we can choose between multiple solutions the most likely connection pathways. For example in brain fiber tracking, the most likely connection pathways are the ones which correspond best to the underlying real fibrous structure. In the case of having more than one geodesic between two points, the pathways can be sorted by indexing them with connectivity value obtained for each one.

One advantage of our algorithm is that it gives the possibility of applying different cost functions in a fast post-processing procedure. Another advantage is the capability of capturing the possible multi-path connections between two given points. In order to show the potential of the algorithm for fiber tracktography, we apply it to two dimensional synthetic data.

2. Governing Equation

In this section we present the governing equations for computing geodesics. A geodesic connecting a pair of points on a Riemannian manifold embedded in $\mathbb{R}^2$ is defined as a curve $\mathbf{u}(\tau) = (u(\tau), v(\tau))^\top$ extremizing the length functional

$$L(\mathbf{u}) = \int_0^{\mathcal{T}} (\dot{\mathbf{u}}^\top G \dot{\mathbf{u}})^{1/2} d\tau \,, \tag{1}$$

where $G = G(\mathbf{u}(\tau))$ is the Riemannian metric. The parameters (u, v) belong to a two dimensional bounded set $\Omega \subset \mathbb{R}^2$ and specify the location of the geodesic, and τ is a parameter along the geodesic. Geodesics are given by a system of two second order ODEs on Ω [7],

$$\begin{aligned} \ddot{u} + \Gamma^1_{11}\dot{u}^2 + 2\Gamma^1_{12}\dot{u}\dot{v} + \Gamma^1_{22}\dot{v}^2 = 0, \\ \ddot{v} + \Gamma^2_{11}\dot{u}^2 + 2\Gamma^2_{12}\dot{u}\dot{v} + \Gamma^2_{22}\dot{v}^2 = 0. \end{aligned} \tag{2}$$

Here the dot denotes differentiation with respect to τ and $\Gamma^k_{ij}(u, v)$ are Christoffel symbols defined by

$$\Gamma^k_{ij} = \sum_{m=1}^{2} \frac{1}{2} g^{km}[(g_{jm})_i + (g_{im})_j - (g_{ji})_m], \tag{3}$$

where (g_{ij}) denotes the matrix component of G and (g^{ij}) the ones of G^{-1}. In DTI applications, the metric G is the inverse of the diffusion tensor D. Subscripts 1 and 2 on the r.h.s. indicate differentiation with respect to u and v, respectively.

We reduce equation (2) to three first order ODEs by setting

$$\dot{u} = \frac{du}{d\tau} = \cos\theta, \qquad \dot{v} = \frac{dv}{d\tau} = \sin\theta, \tag{4}$$

and therefore $\dot{v} = \dot{u}\,\tan\theta$. Differentiating with respect to τ gives us

$$\ddot{v} = \ddot{u}\,\tan\theta + \dot{u}\frac{1}{\cos^2\theta}\dot{\theta}. \tag{5}$$

Now let $\gamma = (u, v, \theta)^\top$. Using (5) and (2) we have

$$\dot{\theta} = \sin\theta(\Gamma^1_{11}\cos^2\theta + 2\Gamma^1_{12}\cos\theta\sin\theta + \Gamma^1_{22}\sin^2\theta) - \cos\theta(\Gamma^2_{11}\cos^2\theta + 2\Gamma^2_{12}\cos\theta\sin\theta + \Gamma^2_{22}\sin^2\theta) =: \rho(\gamma).$$

Therefore the system of ODEs (2) for geodesics reads

$$\dot{\gamma} = \mathbf{g}(\gamma) := \begin{pmatrix} \cos\theta \\ \sin\theta \\ \rho(\gamma) \end{pmatrix}, \tag{6}$$

Note that by the particular choice of (4) we identify τ with the *Euclidean* arc length parameter.

3. Two-Point Ray Tracing

By equation (6) we can compute all possible geodesics starting at an initial point and ending at some point on the domain. We concentrate on the problem of computing geodesics between two given points inside the boundary. In order to tackle this problem we first solve (6) for these two given points as initial locations and all initial directions in a discrete domain. This gives us two sets of geodesics starting at these two points and ending at the boundary. We then post-process these solutions to obtain the geodesics between the two points. This procedure is called two-point ray tracing [15].

We consider the triplet $\gamma_0 = (u_0, v_0, \theta_0)^\top$ as a point in the space $\Omega_p = \Omega \times \mathbb{S}$, where $\mathbb{S} = [0, 2\pi)$. Let $F(\gamma_0) = (U, V, \Theta)^\top$ be the *escape point* of the geodesic satisfying (6) and starting at γ_0, i.e., $F(\gamma_0)$ is the point where the geodesic starting at $(u_0, v_0) \in \Omega$ with direction $\theta_0 \in \mathbb{S}$ crosses the boundary of Ω at (U, V) with direction $\Theta \in \mathbb{S}$, see Figure 1. Moreover, let $T(\gamma_0)$ be the Euclidean length of the geodesic between the starting point and the corresponding escape point. We call $T(\gamma_0)$ the *escape length*. We note that given an initial point γ_0 we can compute $F(\gamma_0)$ and $T(\gamma_0)$ by solving (6) using an ODE solver such as the fourth order Runge-Kutta method.

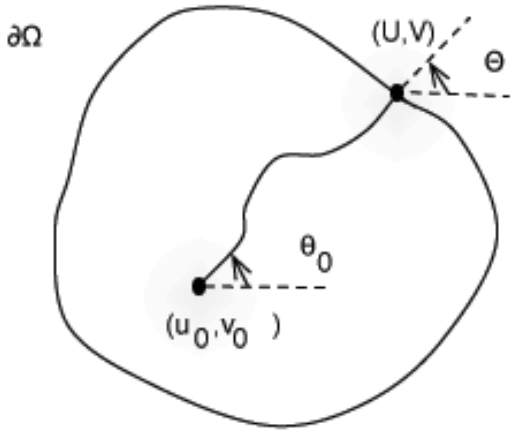

Figure 1. A geodesic in the parameter space. The function F is defined as $F(u, v, \theta) = (U, V, \Theta)$.

Now suppose we want to find all possible geodesic paths between two points (u_1, v_1) and (u_2, v_2) in Ω. We first observe that $F(\gamma_1) = F(\gamma_2)$ if and only if the points $\gamma_1 = (u_1, v_1, \theta_1)^\top$ and $\gamma_2 = (u_2, v_2, \theta_2)^\top$ lie on the same geodesic. We can thus find θ_1 and θ_2 as the solution to

$$F(u_1, v_1, \theta_1) = F(u_2, v_2, \theta_2). \tag{7}$$

There maybe multiple solutions to (7) giving multiple geodesics. The Euclidean length of the geodesic connecting these two points is then given by $\mathcal{T} = |T(\gamma_1) - T(\gamma_2)|$.

In order to solve (7) we note that, since $F = (U, V, \Theta)^\top$ is a point on the boundary $\partial\Omega_p$, it can be reduced to a point $(S, \Theta) \in \mathbb{R}^2$, where S represents the escape location on the boundary. For example in a rectangular domain Ω we choose $S \in [0, 2\pi]$ along $\partial\Omega$, see Figure 2a. The left and right hand sides of (7) are therefore curves in $\mathbb{R}^2$ parameterized by θ_1 and θ_2, [12]. Solving (7) amounts to finding crossing points of these curves, see Figure 2b.

Numerically, we first solve the geodesic equation (6) for the initial points (u_1, v_1, θ^k) and (u_2, v_2, θ^k) where $\theta^k = k\triangle\theta$ and $\triangle\theta = \frac{2\pi}{N}$. Discretizing the computational domain Ω into N^2 points, the complexity of solving the ODEs for two initial points (u_1, v_1) and (u_2, v_2) with N initial directions is $O(N^2)$. Having the discrete solutions (escape points and escape lengths) for the initial points (u_1, v_1) and (u_2, v_2) with all N directions we find the crossing points of two curves of N straight line segments. This can be done with a complexity of $O(N)$, [17]. Therefore the total complexity of finding all possible geodesics between M pairs of points will be $O(M\,N^2)$.

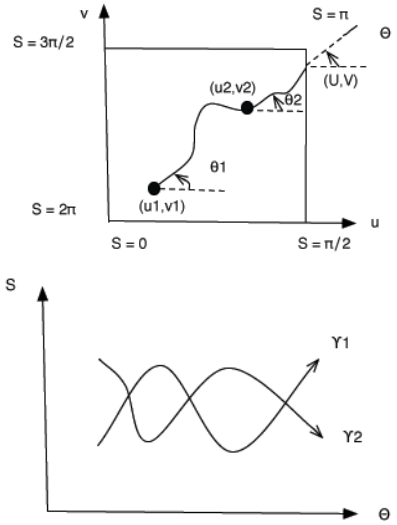

Figure 2. A geodesic in the parameter space, starting at point $\gamma_1 = (u_1, v_1, \theta_1)^\top$ and ending at the escape point $F(\gamma_1) = (U, V, \Theta)^\top$. In a discrete case, curves in Figure (b) contain N straight line segments.

4. Numerical Examples

In this section, we apply the two-point ray tracing method to compute all possible geodesics in a tensor-warped field. We present the method on two different computational fields. The main difference between these two fields is that in the first one we have a continuous tensor field expressed in analytic form. Therefore we can compute the metric derivatives and Christoffel symbols analytically as we integrate equation (6). In the second one, we have a discrete tensor field only at grid points. In order to find the metric derivatives at any point in the domain, we interpolate component-wise the metric derivatives at the grid points.

4.1. Example 1

We consider a two dimensional metric field

$$G = \begin{pmatrix} g_{11} & g_{12} \\ g_{21} & g_{22} \end{pmatrix},$$

where

$$g_{11} = 2\pi^2 \sin^2(\pi v)\,(1 + \sin^2(2\pi u)),$$
$$g_{12} = g_{21} = -\frac{3}{8}\pi^2 \sin(4\pi u)\,\sin(2\pi v),$$
$$g_{22} = \pi^2 (1 - \frac{3}{4}\sin^2(2\pi u)\cos^2(\pi v)),$$

in a rectangular domain $\Omega = [0,1] \times [0.1, 0.9]$. The diffusion tensor is $D = G^{-1}$. Differentiating G with respect to u and v and using (3) gives us the required Christoffel symbols.

Figure 3a shows the geodesic paths for two initial points $(u_1, v_1) = (0.3, 0.6)$ and $(u_2, v_2) = (0.8, 0.2)$ with $N = 50$ initial directions $\theta^k \in \mathbb{S}$, $k = 1, 2, \ldots, N$. Figure 3b shows two intersecting curves in the (S, Θ)-plane corresponding to all geodesics starting at the two initial points. There are two crossing points which determine two geodesics connecting these two points. The two geodesics are in fact the same(in this case) and lie on top of each other, indicate by the bold line in Figure 3a.

4.2. Example 2

In this section, we consider a discrete two dimensional synthetic tensor field. Isotropic tensors are defined as a background (excluding the effects of noise) and anisotropic tensors form curved fibers. The shape of the tensors in the spatial domain represents a section of U-fiber bundle structure. To examine the method for noisy data gaussian noise

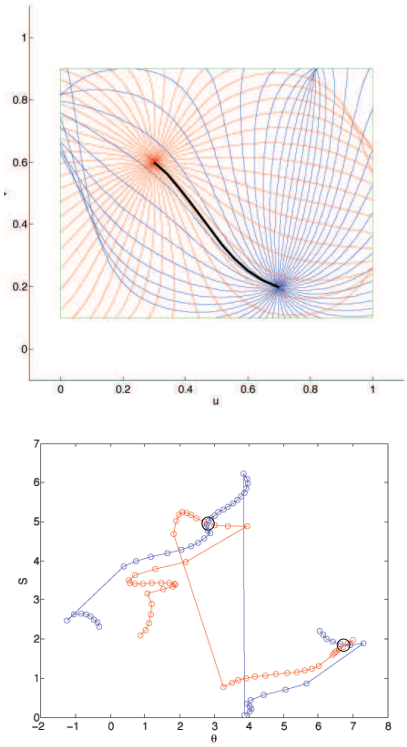

Figure 3. Left figure shows geodesics starting from given initial points and ending at boundaries and the geodesics connecting these two points. Right figure shows two crossing curves. Each curve corresponds to all escape points and escape angles starting from an initial point. The two crossing points are shown by circles around.

is added to each eigenvalue and eigenvector of the diffusion tensors, independently, see Figure 4.

We discretize the computational domain $\Omega = [0,1]^2$ uniformly with the step sizes $\triangle u = \triangle v = \frac{1}{N}$ and grid points $u_i = i\triangle u$, $v_j = j\triangle v$, $i, j = 0, 1, \ldots, N$. Here N is the number of grid points in each direction. Each grid point (u_i, v_j) in this domain is labeled by a two-dimensional tensor $G_{ij} = D_{ij}^{-1}$.

To compute the metric derivative in each grid point we use a finite difference scheme such as the second order central difference

$$\frac{\partial G_{i,j}}{\partial u} \approx \frac{G_{i+1,j} - G_{i-1,j}}{2\triangle u}, \quad \frac{\partial G_{i,j}}{\partial v} \approx \frac{G_{i,j+1} - G_{i,j-1}}{2\triangle v}. \tag{8}$$

We apply the second order one-sided difference scheme for

the grid points situated on the boundaries

$$\frac{\partial G_{0,j}}{\partial u} \approx \frac{-3G_{0,j} + 4G_{1,j} - G_{2,j}}{2\triangle u},$$
$$\frac{\partial G_{N,j}}{\partial u} \approx \frac{3G_{N,j} - 4G_{N-1,j} + G_{N-2,j}}{2\triangle u}.$$

Similar formulations hold for derivatives with respect to v. In order to obtain derivatives needed for computing Christoffel symbols in any point in the domain we apply component-wise interpolation.

Figure 4 shows the two geodesic paths between two initial points $(u_1, v_1) = (0.3, 0.5)$ and $(u_2, v_2) = (0.75, 0.57)$, obtained by the algorithm, using diffusion tensor. It shows that the geodesic with the shortest length between two points (black-curve) does not always follow better fibrous structure, i.e., the U-fiber bundle. This test shows the robustness of the algorithm to noise. The two-point ray tracing algorithm gives the possibility of finding all possible geodesics between two points. In contrast existing methods would calculate just the unique optimal path. Getting the desired path in these methods can be very sensitive to the choice of the cost function using for optimizing the pathways. In the next section, we will show one of the applications of the algorithm to find the geodesic among all geodesics between two points that better coincides with the fibrous structure by using connectivity measurement. Note that in some cases it can be that both geodesic connections are physically meaningful, See for example [13].

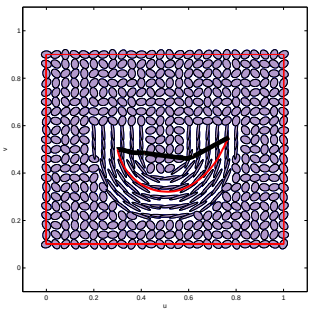

Figure 4. Geodesics computed for synthetic DT fields modeling a curved fiber tract. This figure shows diffusion tensor field with gaussian noise.

5. An Application to Connectivity Measurements

In order to find a neural fiber bundle connecting two given points, we need suitable connectivity measurements to select the optimal geodesic among all possible geodesics between these two points. Recently [1, 16] presented new measurements to assess the degree of connectivity of geodesic paths. In this section, we briefly review these measurements, and apply them to our numerical examples.

A geodesic connecting a pair of points on a Riemannian manifold is defined as a curve $\mathbf{u}(\tau) = (u(\tau), v(\tau))^\top$ extremizing the length functional equation (1).

where $G = G(\mathbf{u}(\tau))$ is the Riemannian metric. The ratio of lengths given by the Euclidean and diffusion induced Riemannian metric tensors $G = D^{-1}$ can be considered as a measure for the connection strength of a geodesic. The proposed measure is given by

$$m_L(\mathbf{u}) = \frac{\int_0^{\mathcal{T}} (\dot{\mathbf{u}}^\top \dot{\mathbf{u}})^{1/2}\, d\tau}{\int_0^{\mathcal{T}} (\dot{\mathbf{u}}^\top G \dot{\mathbf{u}})^{1/2}\, d\tau}, \tag{9}$$

(10)

For the optimal geodesic coinciding with a neural fibrous structure, the measure in (9) is larger compared to the one for other geodesics. Note that (9) can be interpreted as inverse Euclidean-length averaged diffusivity along the curve.

We note that in the neighborhood of the point $\mathbf{u}_0 = \mathbf{u}(0)$ the limit of measurements in (9) as $\mathcal{T} \to 0$ gives the following local measurement

$$M_L(\dot{\mathbf{u}}_0) = \frac{(\dot{\mathbf{u}_0}^\top \dot{\mathbf{u}}_0)^{1/2}}{(\dot{\mathbf{u}}_0^\top G(\mathbf{u}_0)\, \dot{\mathbf{u}}_0)^{1/2}}, \tag{11}$$

where $M_L(\dot{\mathbf{u}}_0) = m_L(\mathbf{u}_0)\ \dot{\mathbf{u}}_0^+$ and λ^+ be the principal eigenvector and the largest eigenvalue of $D(\mathbf{u}_0)$, respectively, and therefore $\dot{\mathbf{u}}_0^+ = \lambda^+ G(\mathbf{u}_0)\dot{\mathbf{u}}_0^+$. By (11) we then have

$$M_L(\dot{\mathbf{u}}_0^+) = (\lambda^+)^{1/2},$$

implying that *locally* the measurements give maxima in the direction of the principal eigenvector of the diffusion tensor, indeed a reasonable local connectivity measure.

We apply the measure (9) to the problem in Section 4.2 with the synthetic data. We get $m_L = 5.23$ and $m_L = 1.45$ for the geodesics showed by (red) and (black) in Figure 4, respectively. Here it can be seen that connectivity of the geodesic coinciding with the fiber bundle are larger than the one of the other geodesic.

6. Discussion and Conclusion

Common approaches for fiber tracking in diffusion tensor imaging based on geodesics give only a single geodesic representing the fiber pathway between two points. This geodesic may not represent the appropriate connecting path. Moreover, there might be multiple pathways which can not be detected by such approaches. We have modified a ray tracing algorithm for computing geodesics in a two-dimensional tensor-warped space. In this approach we obtain all possible geodesics between two given points. One main application of this method is to cases where there are multiple connections between two points in the diffusion tensor field. Furthermore, we can apply different connectivity measurements in order to select the geodesic with the strongest connectivity among all geodesics, in the case just one geodesic is expected.

In this paper, the method is presented to develop an exact algorithm for the fiber tractography. We made use of the second order diffusion tensor data which is still the most commonly used. We applied the algorithm to two dimensional synthetic tensor fields as a proof of concept.

In future work we will extend the algorithm to three dimensions and will apply it to real brain diffusion tensor images. Another future research direction is extending the algorithm to region-region tracking. It is also interesting to investigate how often the multiple geodesics appear in the brain and give the more accurate results.

Acknowledgements.

The Netherlands Organisation for Scientific Research (NWO) is gratefully acknowledged for financial support.

References

[1] L. J. Astola, L. M. J. Florack, and B. M. ter Haar Romeny. Measures for pathway analysis in brain white matter using diffusion tensor imaging. *In Proceeding of Information Processing in Medical Imaging, Lecture Notes in Computer Science*, 2007.

[2] P. Basser, S. Pajevic, C. Pierpaoli, J. Duda, and A. Aldroubi. In vivo fiber tractography using DT-MRI data. *Magnetic Resonance in Medicine*, 44:265–632, 2000.

[3] P. J. Basser and C. Piepaoli. Microstructural and physiological features of tissues elucidated by quantitative-diffusion-tensor MRI. *Journal of Magnetic Resonance*, 111(1):209–219, 1996.

[4] L. O. Donnell, S. Haker, and C. F. Westin. New approaches to estimation of white matter connectivity in diffusion tensor MRI: Elliptic PDEs and geodesics in a tensor-warped space. *International Conference on Medical Image Computing and Computer-Assisted Intervention - MICCAI'02*, 2488:459–466, 2002.

[5] M. Jackowski, C. Kao, M. Qui, R. Constable, and L. Staib. White matter tractography by anisotropic wavefront evolution and diffusion tensor imaging. *Medical Image Analysis*, 9:424–440, 2005.

[6] Z. Jun, J. Hao, K. Ning, and C. Ning. Fiber tractography in diffusion tensor magnetic resonance imaging: A survey and beyond. *Department of Computer Science, University of Kentucky, USA*, 2005.

[7] J. Keller and R. M. Lewis. Asymptotic methods for partial differential equations: the reduced wave equation and Maxwell's equations. *Surveys of Applied Mathematics*, 1:1–82, 2005.

[8] A. Lenglet, R. Deriche, and O. Faugeras. Inferring white matter geometry from diffusion tensor MRI: application to connectivity mapping. *Proceedings of the Eighth European Conference on Computer Vision*, 3021.

[9] J. Melonakos, V. Mohan, M. Niethammer, K. Smith, M. Kubicki, and A. Tannenbaum. Finsler tracktography for white matter connectivity analysis of the singulum bundle. *MICCAI, Springer*, 2007.

[10] J. Melonakos, E. Pichon, S. Angenent, and A. Tannenbaum. Finsler active contour. *IEEE Transactions on pattern analysis and machin intelligence*, 2007.

[11] S. Mori, S. Wakana, P. v. Zijl, and L. Nagae-Poetscher. MRI atlas of human white matter., 2005. Elsvier, Berlin (2005).

[12] M. Motamed and O. Runborg. A fast phase space method for computing creeping rays. *Journal of Computational Physics*, 219(1):276–295, 2006.

[13] G. Parker, S. Luzzi, D. Alexander, C. Wheeler-Kingshott, O. Ciccarelli, and M. Lambon-Ralph. Lateralization of ventral and dorsal auditory-language pathways in the human brain. *NeuroImage*, 24:656–666, 2007.

[14] G. J. M. Parker, C. A. M. Wheeler-Kingshott, and G. J. Barker. Distributed anatomical brain connectivity derived from diffusion tensor imaging. *Information Processing in Medical Imaging 17th International Conference*, 2482:106–120, 2001.

[15] V. Pereyra, W. H. K. Lee, and H. B. Keller. Solving two-point seismic ray tracing problems in a heterogeneous medium. *Bulletin of the Seismological Society of America*, 70:79–99, 1980.

[16] E. Prados, S. Soatto, C. Lenglet, J. P. Pons, N. Wotawa, R. Deriche, O. Faugeras, and S. Soatto. Control theory and fast marching techniques for brain connectivity mapping. *IEEE computer society press*, 1(1):1076–1083, 2006.

[17] G. Taylor. Another look at the line intersection problem, 1989.